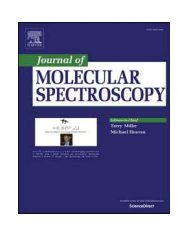
ELSEVIER

Contents lists available at ScienceDirect

Journal of Molecular Spectroscopy

journal homepage: www.elsevier.com/locate/yjmsp





Ammonia – Formic acid complex: internal rotation analysis, calculations, and new microwave measurements

Kristen K. Roehling, Rhett P. Hill, Adam M. Daly, Stephen G. Kukolich *

Department of Chemistry and Biochemistry, University of Arizona, 1306 E. University Avenue, Tucson, AZ 85721, USA

ARTICLE INFO

Keywords:
Hindered Rotation
Hydrogen Bonding
Microwave Spectroscopy
Quadrupole Coupling
Molecular structure

ABSTRACT

New analysis and spectra are reported for the gas-phase ammonia-formic acid complex. Calculations to determine the theoretical barrier to internal rotation were conducted and led to the new internal rotation analysis of the dimer. Using the new analysis and calculations, 12 new lines were measured and assigned and included in the present analysis. This is the first internal rotation analysis for this complex. The measurements were made in the 7–22 GHz range using two Flygare-Balle type pulsed beam Fourier transform microwave (FTMW) spectrometers. The complex was analyzed as a hindered rotor and 20 A and 16 E state transitions were fit with the XIAM5 program. The rotational constants were determined to have the following values: A = 11970.19(9) MHz, B = 4331.479(4) MHz, and C = 3227.144(4) MHz. Rotational constants, quadrupole coupling constants, and internal rotor parameters were fit to the spectrum. Double resonance was used to verify line assignments and access higher frequencies. The barrier to internal rotation was found to be 195.18(7) cm $^{-1}$. High level calculations are in good agreement with experimental values. The calculated V_3 barrier values range from 168.3 to 212.8 cm $^{-1}$.

1. Introduction

Microwave spectroscopy has been used to study large amplitude motion in the gas phase due to the ability to characterize barrier heights. Hindered internal rotation has been previously observed for a variety of rotors. Examples include methyl rotors[1–6], hydroxyl rotors [4,7,8], thiol rotors [8], and ammonia rotors[9–13]. Examples of internal rotation in ammonia heterodimers include ammonia-water [11,12], ammonia hydrogen sulfide [13], ammonia-carbon dioxide [9], ammonia-methanol [14], and ammonia-nitrous oxide [10]. More references for ammonia heterodimers were listed by Stew Novick [15]. In many of these studies, ammonia was determined to be nearly a free rotor with barriers of 12.5 cm $^{-1}$ for NH $_3$ -N $_2$ O 10 and 10.5 cm $^{-1}$ for NH $_3$ -H $_2$ O 11 . These studies provide more information about long-range hydrogen bonding interactions and barriers to internal rotation.

Ammonia and formic acid are good representative molecules to study the weak interactions between carboxylic acids and nitrogen bases in the gas phase. Ammonia dimer has been the subject of multiple microwave spectroscopy studies [16–18], showcasing ammonia's hydrogen bonding ability. The ammonia dimer has also been observed in VRT spectra [19] and calculations published [20]. Current models have difficulty characterizing weak interactions important in many hydrogen-

bonded systems [15]. Providing experimental results in complexes like those between ammonia and formic acid is crucial to improving molecular models, which can then be applied to other systems.

Previous measurements of ammonia-formic acid dimer have been obtained using infrared spectroscopy, characterizing the complex as singly-hydrogen bonded [21]. Our previous measurements of this dimer in the microwave range [22] showed two internal motion states and were interpreted as evidence for large amplitude internal motion. It was not clear at the time whether the motion was due to concerted proton tunneling or hindered internal rotation. Many predicted transitions were missing from the spectrum, and further experimentation was pursued to explain the data. This became an interesting interplay between the experiments and calculations. The calculations predicted a fairly low internal rotation barrier for NH₃ rotation relative to the formic acid frame. Analysis of previously measured [21] transitions led to predictions of many more transitions. We now include 12 new lines associated with the A and E internal rotation states in the analysis below. The present work details an analysis of the torsion-rotation spectrum of the formic acid ammonia complex. No previous internal rotation analysis has been published for this complex. (See Fig. 1).

E-mail address: kukolich@arizona.edu (S.G. Kukolich).

^{*} Corresponding author.

2. Computational

New high-level calculations were done for the FA-NH₃ complex to obtain vibrationally averaged structures, rotational constants and quadrupole coupling parameters. Calculations were also made for the hindered internal rotation of the NH₃ molecule in the complex. Computations were performed on the University of Arizona HPC Puma system using Gaussian G-16 [23] with 94 cores and using 470 GB of memory. Methods were chosen which gave good structural parameters in previous microwave work. The methods were MP2 [24] and DFT with B3LYP[25] and M11 [26] and CCSD [27]. The basis sets were aug-cc-pVQZ [28], cc-pVQZ[29], and def2QZvpp [30]. For B3LYP, slightly better results were obtained using the "EmpiricalDispersion = GD3" keyword. For the Gaussian-16 suites (G-16), the keyword "output = picket" provided microwave parameters, A, B, C, and quadrupole coupling constants for N-14. The vibrationally averaged parameters are obtained using the keyword "freq = anharm".

For the internal rotation calculations, the dihedral angle O2-O1-N1-H4 was scanned from 0 to 360 degrees with optimization with the dihedral fixed. The energy plot obtained from this scan is shown in Fig. 2. This shows a V_3 , 3-fold barrier to the internal rotation.

This scan, using B3LYP/aug-cc-PVQZ EmpiricalDispersion = GD3 yields a V_3 barrier of 212.8 cm $^{-1}$. From the M11/def2Vpp calculation the V_3 barrier is 212 cm $^{-1}$. For MP2/aug-cc-pVQZ the calculated barrier is 168.3 cm $^{-1}$.

The calculated rotational constants and other parameters of interest are provided in Table 1. The equilibrium rotational constants are $A_e,\,B_e$ and C_e and vibrational averaged (v = 0) values $A_0,\,B_0$ and C_0 . The method B3LYP with the aug-cc-pVQZ basis set with GD3 empirical dispersion for the v = 0 vibrational state yielded estimates of ammonium formate rotational constants closest to the experimental values. The vibrational averaged values were obtained using freq = anharm in the G-16 calculations. Vibrational averaging for the v = 0 level improved the results for the B3LYP and M11 calculations.

The calculated barrier to concerted proton tunneling using B3LYP/aug-cc-pVQZ-GD3 is 3395 cm⁻¹. Since this barrier is substantially higher than the internal rotation barrier, it now appears that the previous discrepancies and extra features in the spectrum are due to the internal rotation. For comparison the barrier to proton tunneling in the simplest carboxylic acid system studied, DCOOH—HCOOH, was calculated to be 2500 cm⁻¹ [31].

3. Experimental

A hindered rotation analysis of the previously measured transitions

was made using the XIAM5 program [32], which is an improved version of the original XIAM [33] program. Using results from this fit, searches were made for new internal rotor transitions. Microwave measurements were made using Flygare-Balle-type spectrometers as described in the previous ammonia-formic acid paper [16]. Direct measurements were made in the 14–17 GHz range and double resonance measurements were made between 15 and 22 GHz. We have measured, assigned and included 12 new lines associated with the A and E internal rotation states in the analysis.

A brief description of the experiment is given here. A sample of commercially available ammonium formate was heated in a glass cell to $40{\text -}50\,^{\circ}\text{C}$ under 1 atm of argon. At a rate of 2 Hz, the sample was injected into a pulsed beam microwave cavity. Direct measurements were first made at 14.3 GHz. For the current data collection routine, several hundred valve pulses were obtained for each line spectrum. For our multi-FID program we use 4 acquisitions per valve pulse. An acquisition can be defined as a microwave stimulating pulse followed by the recorded free induction decay signal. A representative spectrum is given in Fig. 3. Due to the double side band detection, signals were obtained from lines above and below the stimulating signal. Experimental linewidths are typically 20 KHz, but the lines in Fig. 3 are 40 kHz wide from partially resolved structure.

Double resonance was used to detect the b-dipole transition predicted to be at $15.1~\mathrm{GHz}.$ While monitoring $7564.591~\mathrm{MHz}$ (A state: $1_{01}F=1\rightarrow0_{00}F=0$), two characteristic interference signals were observed at 15240.52(10) and 15240.84(10) MHz corresponding to connections made with the same ground state $(0_{00}F=0).$ These transitions are shown in Fig. 4, and listed in Table 2. The reported signal is the ratio of integrated area of the pump signal (monitored signal 7564.591 MHz) with the probe frequency off to the signal ratio with probe frequency on. This ratio is close to one off resonance and exceeds one as we near resonance. The pump signal is reduced on resonance. Steps of 1 kHz, 20 acquisitions per step at the monitored frequency were used to construct Fig. 4.

Efforts to measure this transition for the E-state were unsuccessful. It is believed that nearby modes at 14.6 GHz interfere with this double resonance acquisition.

Measured transitions are listed in Table 2 and include 20 A-symmetry type and 16 E-symmetry type. Both a-dipole and b-dipole transitions were found, but no c-dipole transitions.

4. Analysis

The assignments included in our previous work on the complex were used as the starting point for the current measurements. Using the previously fitted rotational constants and the calculated values for F0, delta,

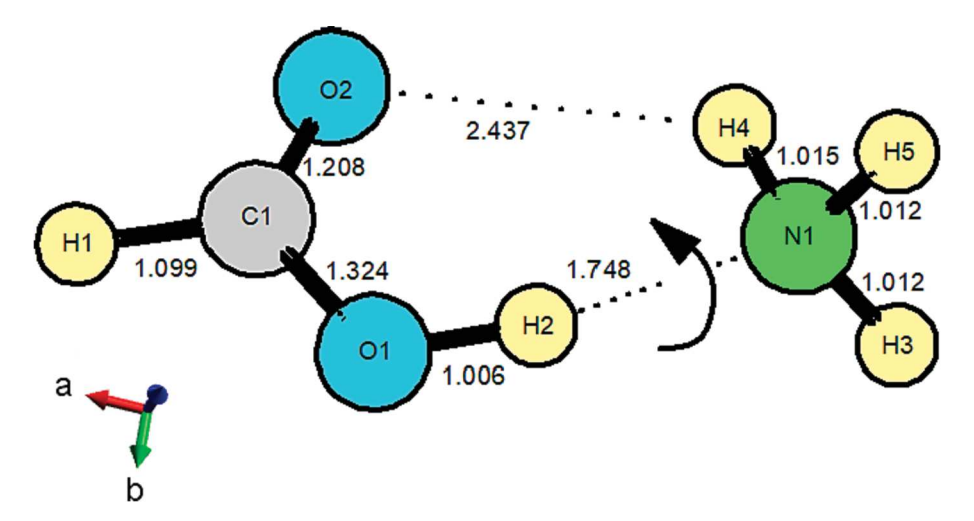


Fig. 1. Structure of the FA-NH3 complex showing the NH₃ internal rotation axis. The complex is shown in Fig. 1. The principal axes are shown, a-red, b-green, c-blue. (For interpretation of the references to colour in this figure legend, the reader is referred to the web version of this article.)

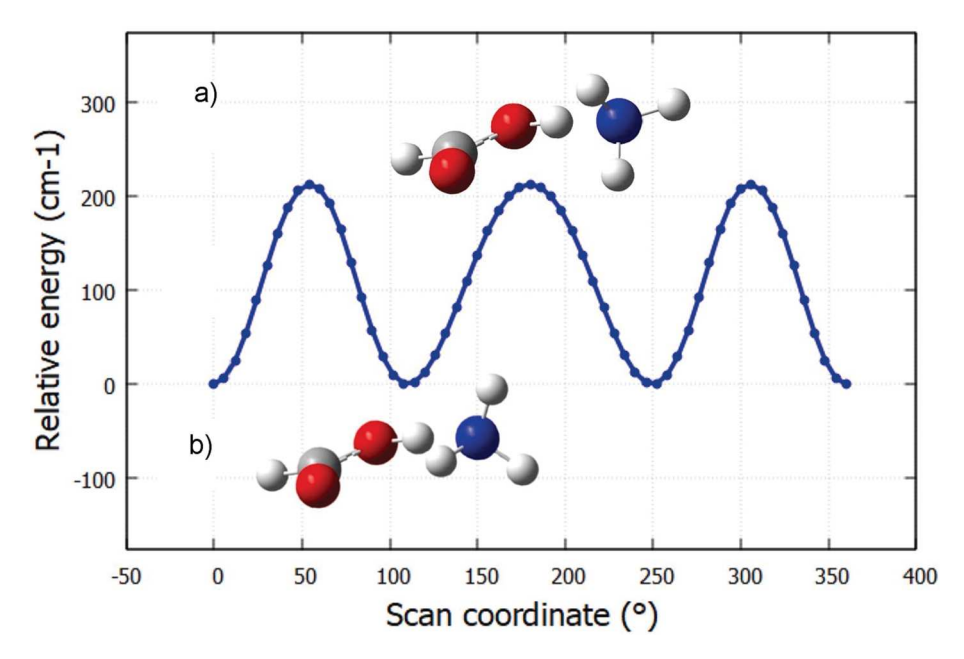


Fig. 2. Energy scan plot for the dihedral angle O2-O1-N1-H4. a) shows the higher energy rotamer and b) shows the minimum energy rotamer.

Table 1 The experimental and calculated parameters of ammonium formate. Frequencies are in MHz. 31 transitions were fit. The equilibrium rotational constants are A_e , B_e and C_e and vibrational averaged (v = 0) values A_0 , B_0 and C_0 . 1. Experimental column gives results of the XIAM5 fit. GD3 is for Empiracal Dispersion = GD3.

-	0 ' '	0 1	O		1 1	
Parameter	1. Experimental	2. B3LYP	3. M11	4. MP2	5. MP2	6. CCSD
Basis set	_	aug-cc-pVQZ-GD3	def2-QZVPP	cc-pVQZ	aug-cc-pVQZ	aug-cc-pVDZ
Ae	_	11931.447	11964.172	11887.191	11881.504	11733.019
Be	_	4426.4507	4510.546	4495.098	4489.216	4275.553
Ce	_	3285.3285	3334.325	3318.898	3315.347	3187.103
A_0	11970.19(9)	11953.052	11954.810	_	11922.622	_
B_0	4331.478(4)	4347.711	4443.811	_	4385.406	_
C_0	3227.144(4)	3238.220	3291.526	_	3255.584	_
$1.5 \chi_{aa}$ (N)	-0.960(14)	-0.7650	-0.639	-0.660	- 0.6695	-0.798
$0.25(\chi_{bb}-\chi_{cc})(N)$	-0.7155(63)	-0.925	-1.0383	-0.859	-0.839	0.789
$X_{ab}(N)$	Fixed 2.7	2.73521	2.935	2.529	2.488	-2.478
μ_a (Debye)	_	2.557	2.324	2.515	2.489	2.361
μ _b (Debye)	_	0.320	0.356	0.191	0.225	0.259
μ _c (Debye)	_	0.0001	0.0002	0.0004	0.0006	0.0005
V ₃ (cm-1)	195.18(7)	212.8	211.8	_	168.3	_
σ(kHz)	13.2	_	_	_	_	_

and the V $_3$ barrier, the internal rotor spectrum was predicted using XIAM [28]. The predicted value for the E state $2_{12} \rightarrow 1_{11}$ transition was used to locate the missing transition. Using the previous two-state fit, the E state $2_{12} \rightarrow 1_{11}$ was predicted at 14015 MHz, while XIAM predicted the transition at 14200 MHz. The region of 13485–14596 MHz was scanned, and a signal showing quadrupole splitting at 14308 MHz was the closest transition to the predicted E state $2_{12} \rightarrow 1_{11}$. The signal at 14308 MHz was directly measured and used in the internal rotor fit to predict the E state $2_{11} \rightarrow 1_{10}$ at 15919 MHz. When the surrounding region was scanned, a signal with quadrupole splitting was located at 15923 MHz.

The initial internal rotor prediction estimated the A state $0_{00} \rightarrow 1_{11}$ transition at 15241 MHz. For some transitions,the internal rotor prediction does not vary significantly from the two-state prediction which places the transition at 15244 MHz. Previous searches for the transition were unsuccessful due to the insufficient strength of the b-dipole at about 0.2 Debye. Only noise spectra were seen using the normal single-resonance method in this region. New double resonance measurements located the transition at 15241 MHz.

A final internal rotor fit was made using XIAM5 containing 20 transitions in the A state and 16 transitions in the E state. The transitions include a-dipole and b-dipole lines measured directly or by double resonance. Double resonance was primarily utilized to observe weak b-

dipole transitions or a-dipole frequencies out of our capabilities for direct measurement. Double resonance also verified a-dipole assignments originally. The fitted parameters obtained from the analysis are shown in Table 3.

5. Discussion

The spectra measured for two states of the FA-NH3 complex are assigned to the A and E symmetry states of a V_3 hindered rotor. The fit to the measured spectrum (Table 2) is very good for a hindered rotor. The correlation between V_3 and F0 in the fit is high so uncertainties in those parameters are estimated to be 3σ or greater. The angle delta and top moment I α (1/F0) were obtained from the calculated equilibrium structure and the values are similar to the present experimental values. Calculated values are delta =0.875 rad and F0=186.1 GHz for the equilibrium structure. The deviations could result from wobbling of the top axis relative to the a-axis of the complex. Examining the G-16 scan reveals that the angle delta oscillated between 40° and 50° as the NH3 rotates. This motion can contribute significantly to effective values of delta and F0 in the XIAM5 fit.

The changes in the nitrogen atom electronic environment can be determined by comparing the experimental value of eQq_{aa} to the

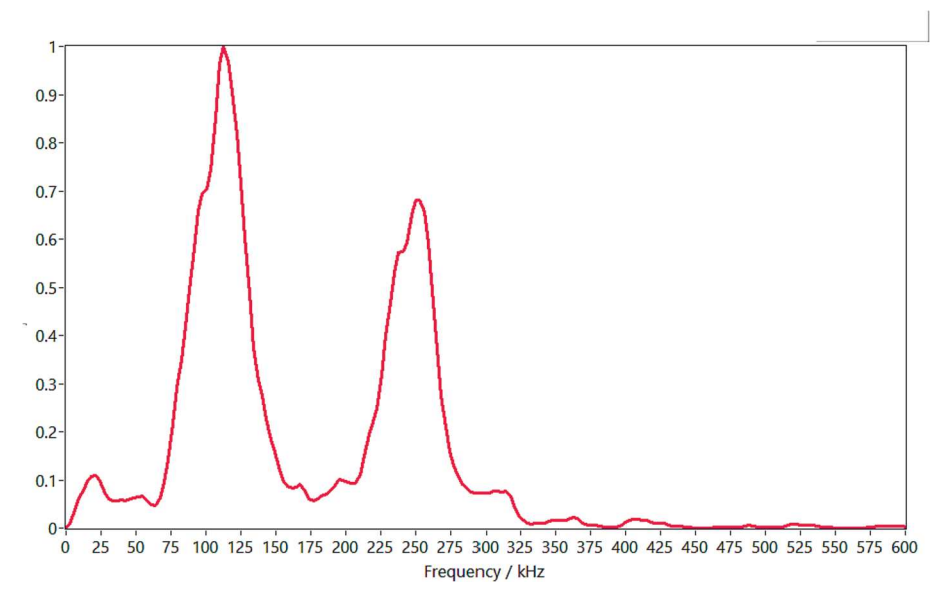


Fig. 3. Two quadrupole components near the stimulation frequency of 14308.200 MHz for the $2_{12} \rightarrow 1_{11}$ E state transition. Line frequencies are 14308.093(10) MHz (F = 2 \rightarrow 1) and 14308.442(10) MHz (F = 3 \rightarrow 2), observed with 150 valve pulses. This is a plot of intensity vs. frequency offset in kHz.

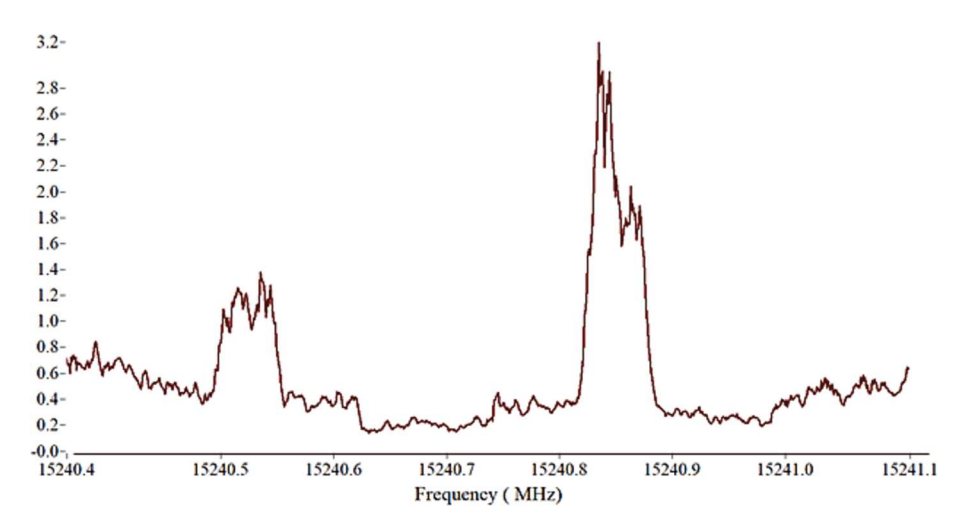


Fig. 4. Two quadrupole components detected by double resonance. Monitoring the A-state $1_{01}F = 1 \rightarrow 0_{00}F = 0$ (7564.591 MHz), scanning the $1_{11}F = 0 \rightarrow 0_{00}F = 0$ (15240.52(10) MHz) and $1_{11}F = 1 \rightarrow 0_{00}F = 0$ (15240.84(10) MHz) transitions. The y-axis is the ratio of the integrated area of the monitored transition (pump signal) without the probe signal to the integrated area of the monitored signal with the probe signal on. The probe frequency is scanned in 1 kHz steps, with 20 acquisitions of the monitored signal per step.

nitrogen experimental quadrupole tensor for ammonia. The experimental value for free NH_3 is $eQq_{cc} = -4.09$ MHz [34]. First, the angle between the c-axis of ammonia and the a-axis of the ammonia-formic acid complex was determined to be 50.14°. This is the same as the angle delta in the XIAM5 fit. Using this angle in the a-b plane of the complex, the ammonia nitrogen quadrupole tensor was rotated from the ammonia principal axis system to the ammonia-formic acid complex principal axis system. This was accomplished with a matrix rotation program (MATROT). The resulting calculated nitrogen quadrupole a-axis component is - 0.63 MHz. This is very close to the experimental eQq_{aa} or $\chi_{aa} =$ -0.640 MHz. The barrier to internal rotation has been fit to 195.18(7) cm⁻¹ which agrees very well with calculations made (168 cm⁻¹ —212 cm⁻¹). This barrier is an order of magnitude smaller than the calculated double proton concerted motion originally proposed to explain the two states observed. The binding energy of the formic-ammonia complex is estimated to be 3395 cm⁻¹.

6. Conclusions

The gas phase ammonia-formic acid dimer was analyzed as a low-barrier internal rotor and further microwave spectroscopy measurements were made. The spectrum reveals hydrogen-bonded dimer with A and E internal rotor states, and 12 new transitions were measured. The V_3 barrier was determined to be 195.18(7) \mbox{cm}^{-1} . The internal rotation axis nearly coincides with the hydrogen bond with the H atom on formic acid. The second hydrogen bond is responsible for the V_3 barrier to the hindered rotation. Double resonance was employed to extend our frequency range and detect weak b-dipole transitions, and to verify assignments.

CRediT authorship contribution statement

Kristen K. Roehling: Writing – review & editing, Writing – original draft, Methodology, Formal analysis, Data curation. Rhett P. Hill: Writing – review & editing, Software, Methodology, Investigation,

Table 2
Quantum numbers and line frequencies (MHz) for the XIAM5 analysis. The 12 newly measured transitions are indicated in the last column by N, previously reported transitions are marked o.

"	J'	K-	K+	J	K-	K+	2F'	2F	Sym	obs (MHz)	o-c(MHz)	error	new
1:	1	0	1	0	0	0	2	2	/A	7564.3975	0.0189	0.010	o
2:	1	0	1	0	0	0	4	2	/A	7564.5911	0.0171	0.010	0
3:	1	0	1	0	0	0	0	2	/A	7564.8857	0.0190	0.010	0
4:	1	K	0	0	K	0	2	2	/E	7539.9712	-0.0192	0.010	0
5:	1	K	0	0	K	0	4	2	/E	7540.1563	-0.0143	0.010	0
6:	1	K	0	0	K	0	0	2	/E	7540.4302	-0.0104	0.010	0
7:	2	0	2	1	0	1	4	4	/A	15016.7239	0.0025	0.010	0
8:	2	0	2	1	0	1	2	0	/A	15016.8560	0.0086	0.010	0
9:	2	0	2	1	0	1	6	4	/A	15016.9908	0.0001	0.010	0
10:	2	0	2	1	0	1	2	2	/A	15017.3354	-0.0002	0.010	0
11:	2	K	0	1	K	0	4	4	/E	14977.1289	0.0132	0.010	0
12:	2	K	0	1	K	0	4	2	/E	14977.2832	-0.0127	0.010	0
13:	2	K	0	1	K	0	6	4	/E	14977.3916	0.0223	0.010	0
14:	2	K	0	1	K	0	2	4	/E	14977.5078	-0.0023	0.010	0
15:	2	K	0	1	K	0	2	2	/E	14977.6982	0.0079	0.010	0
16:	2	1	1	1	1	0	2	2	/A	16238.1576	-0.0004	0.010	N
17:	2	1	1	1	1	0	4	2	/A	16238.7031	-0.0046	0.010	0
18:	2	1	1	1	1	0	6	4	/A	16238.8781	-0.0014	0.010	0
19:	2	1	1	1	1	0	4	4	/A	16239.2254	-0.0074	0.010	N
20:	2	1	1	1	1	0	2	0	/A	16239.4688	-0.0020	0.010	0
21:	2	K	-1	1	K	-1	2	2	/E	15923.4606	0.0073	0.010	N
22:	2	K	-1	1	K	-1	6	4	/E	15923.9505	-0.0014	0.010	N
23:	2	K	-1	1	K	-1	2	0	/E	15924.2813	-0.0094	0.010	N
24:	2	1	2	1	1	1	4	4	/A	14018.2634	-0.0150	0.010	0
25:	2	1	2	1	1	1	4	2	/A	14018.6037	-0.0044	0.010	0
26:	2	1	2	1	1	1	6	4	/A	14018.8262	-0.0148	0.010	0
27:	2	1	2	1	1	1	2	2	/A	14019.4922	0.0089	0.010	0
28:	2	K	1	1	K	1	4	4	/E	14307.9464	0.0077	0.010	N
29:	2	K	1	1	K	1	4	2	/E	14308.0925	-0.0010	0.010	N
30:	2	K	1	1	K	1	6	4	/E	14308.4418	-0.0035	0.010	N
31:	2	K	1	1	K	1	2	2	/E	14308.8750	-0.0066	0.010	N
32:	1	1	1	0	0	0	2	2	/A	15240.5200	-0.0250	0.100	N
33:	1	1	1	0	0	0	4	2	/A	15240.8400	-0.0347	0.100	N
34:	3	1	3	2	1	2	8	6	/A	20960.9500	0.0418	0.100	0
35:	3	0	3	2	0	2	8	6	/A	22252.5300	-0.0044	0.100	0
36:	3	K	0	2	K	0	8	6	/E	22210.1500	0.1762	0.100	N

Table 3 Molecular parameters from the XIAM5 analysis. The standard deviation for the fit is ${\rm SD}=0.013~{\rm MHz}.$

Molecular parameter	Value (error 1 σ)				
A (MHz)	11970.19(9)				
B (MHz)	4331.479(4)				
C (MHz)	3227.144(4)				
F0 (MHz)	217473(89)				
$V_3 \text{ (cm}^{-1})$	195.18 (7)				
F (MHz)	225831.062 {fixed}				
delta (radians)	0.79874 (6)				
D _J (kHz)	9.37(42)				
χ _{aa} (MHz)	-0.6397(95)				
$\chi_{\rm bb}$ - $\chi_{\rm cc}$ (MHz)	-2.862(25)				
χ _{ab} (MHz)	2.7 {fixed}				

Formal analysis, Data curation. **Adam M. Daly:** Writing – review & editing, Supervision, Software, Project administration, Methodology, Investigation, Formal analysis, Data curation. **Stephen G. Kukolich:** Writing – review & editing, Writing – original draft, Project administration, Funding acquisition, Formal analysis, Data curation, Conceptualization.

Declaration of competing interest

The authors declare that they have no known competing financial interests or personal relationships that could have appeared to influence the work reported in this paper.

Data availability

Data will be made available on request.

Acknowledgements

This material is based upon work supported by the National Science Foundation under Grant No. CHE-1952289 at the University of Arizona. We thank Myla Gonzalez and Anushka Desai for help with the data and calculations. We are very grateful to Doug Fox of Gaussian, Inc for much helpful advice on G-16.

References

- V.W. Laurie, Microwave spectrum and internal rotation of ethyl cyanide, J. Chem. Phys. 31 (6) (2004) 1500–1505, https://doi.org/10.1063/1.1730643.
 E. Hirota, Internal rotation in isopropyl alcohol studied by microwave
- [2] E. Hirota, Internal rotation in isopropyl alcohol studied by microwave spectroscopy, J. Phys. Chem. 83 (11) (1979) 1457–1465, https://doi.org/10.1021/ i100474a020.
- [3] T. Nguyen, V. Van, C. Gutlé, W. Stahl, M. Schwell, I. Kleiner, H.V.L. Nguyen, The microwave spectrum of 2-methylthiazole: 14N nuclear quadrupole coupling and methyl internal rotation, J. Chem. Phys. 152 (13) (2020) 134306, https://doi.org/ 10.1063/1.5142857.
- [4] R.K. Kakar, C.R. Quade, Microwave rotational spectrum and internal rotation in gauche ethyl alcohol, J. Chem. Phys. 72 (8) (2008) 4300–4307, https://doi.org/ 10.1063/1.439723.
- [5] S. Baweja, E. Antonelli, S. Hussain, A. Fernández-Ramos, I. Kleiner, H.V.L. Nguyen, M.E. Sanz, Revealing internal rotation and 14N nuclear quadrupole coupling in the atmospheric pollutant 4-methyl-2-nitrophenol: Interplay of microwave spectroscopy and quantum chemical calculations, Molecules 28 (5) (2023) 2153, https://doi.org/10.3390/molecules28052153.
- [6] K.P.R. Nair, S. Herbers, W.C. Bailey, D.A. Obenchain, A. Lesarri, J. Grabow, H.V. L. Nguyen, Internal rotation and chlorine nuclear quadrupole coupling in 2-chloro-4-fluorotoluene explored by microwave spectroscopy and quantum chemistry,

- Spectrochim. Acta A Mol. Biomol. Spectrosc. 247 (2021) 119120, https://doi.org/10.1016/j.saa.2020.119120.
- [7] G. Cazzoli, D.G. Lister, A.M. Mirri, Rotational isomerism and barriers to internal rotation in hydroxyacetonitrile from microwave spectroscopy, J. Chem. Soc., Faraday Trans. 2. 69(0) (1973) 569-578. DOI: 10.1039/F29736900569.
- [8] F. Inagaki, I. Harada, T. Shimanouchi, Far-infrared spectra and barriers to internal rotation of isopropyl alcohol and alkyl mercaptans, J. Mol. Spectrosc. 46 (3) (1973) 381–396, https://doi.org/10.1016/0022-2852(73)90051-9.
- [9] G.T. Fraser, K.R. Leopold, W. Klemperer, The rotational spectrum, internal rotation, and structure of NH3-CO2, J. Chem. Phys. 81 (6) (1984) 2577–2584, https://doi.org/10.1063/1.447965.
- [10] G.T. Fraser, D.D. Nelson Jr, G.J. Gerfen, W. Klemperer, The rotational spectrum, barrier to internal rotation, and structure of NH₃–N₂O, J. Chem. Phys. 83 (11) (1985) 5442–5449, https://doi.org/10.1063/1.449714.
- [11] P.A. Stockman, R.E. Bumgarner, S. Suzuki, G.A. Blake, Microwave and tunable far-infrared laser spectroscopy of the ammonia-water dimer, J. Chem. Phys. 96 (4) (1992) 2496–2510, https://doi.org/10.1063/1.462054.
- [12] P. Herbine, T.R. Dyke, Rotational spectra and structure of the ammonia-water complex, J. Chem. Phys. 83 (8) (1985) 3768–3774, https://doi.org/10.1063/ 1401109
- [13] P. Herbine, T.A. Hu, G. Johnson, T.R. Dyke, The structure of NH₃·H₂S and free internal rotation effects, J. Chem. Phys. 93 (8) (1990) 5485–5495, https://doi.org/ 10.1063/1.459618
- [14] G.T. Fraser, R.D. Suenram, F.J. Lovas, W.J. Stevens, Microwave spectrum of the CH3OH-NH3 complex, Chem. Phys. 125 (1) (1988) 31–43, https://doi.org/ 10.1016/0301-0104(88)85004-3.
- [15] S.E. Novick, Bibliography of Rotational Spectra of Weakly Bound Complexes. (2019). https://wesfiles.wesleyan.edu/home/snovick/SN webpage/vdw.pdf.
- [16] D.D. Nelson Jr, G.T. Fraser, W. Klemperer, Ammonia dimer: A surprising structure, J. Chem. Phys. 83 (12) (1985) 6201–6208, https://doi.org/10.1063/1.449566.
- [17] D.D. Nelson Jr, W. Klemperer, G.T. Fraser, F.J. Lovas, R.D. Suenram, Ammonia dimer: Further structural studies, J. Chem. Phys. 87 (11) (1987) 6364–6372, https://doi.org/10.1063/1.453466.
- [18] J.G. Loeser, C.A. Schmuttenmaer, R.C. Cohen, M.J. Elrod, D.W. Steyert, R. J. Saykally, R.E. Bumgarner, G.A. Blake, Multidimensional hydrogen tunneling dynamics in the ground vibrational state of the ammonia dimer, J. Chem. Phys. 97 (7) (1992) 4727–4749, https://doi.org/10.1063/1.463874.
- [19] R.C. Cohen, R.J. Saykally, Vibration-rotation-tunneling spectroscopy of the van der Waals bond: A new look at intermolecular forces, J. Phys. Chem. 96 (1992) 1024–1040, https://doi.org/10.1021/j100182a006.
- [20] J. Aling, K. Szalewicz, A. v. d. Avoird, Ammonia dimer: extremely fluxional but still hydrogen bonded. Nat. Commun. 13 (2022). DOI: 10.1038/s41467-022-28862-z.
- [21] S. Hellebust, B. O'Riordan, J. Sodeau, Cirrus cloud mimics in the laboratory: An infrared spectroscopy study of thin films of mixed ice of water with organic acids and ammonia, J. Chem. Phys. 126 (8) (2007) 084702, https://doi.org/10.1063/ 1.2464082.

- [22] K.K. Roehling, J.L. Nichols, A.M. Daly, S.G. Kukolich, Microwave measurements, calculations, and analysis for the gas phase ammonia-formic acid dimer, J. Mol. Spectrosc. 393 (2023) 111772, https://doi.org/10.1016/j.jms.2023.111772.
- Gaussian 16, Revision B.01, M. J. Frisch, G. W. Trucks, H. B. Schlegel, G. E. Scuseria, M. A. Robb, J. R. Cheeseman, G. Scalmani, V. Barone, G. A. Petersson, H. Nakatsuji, X. Li, M. Caricato, A. V. Marenich, J. Bloino, B. G. Janesko, R. Gomperts, B. Mennucci, H. P. Hratchian, J. V. Ortiz, A. F. Izmaylov, J. L. Sonnenberg, D. Williams-Young, F. Ding, F. Lipparini, F. Egidi, J. Goings, B. Peng, A. Petrone, T. Henderson, D. Ranasinghe, V. G. Zakrzewski, J. Gao, N. Rega, G. Zheng, W. Liang, M. Hada, M. Ehara, K. Toyota, R. Fukuda, J. Hasegawa, M. Ishida, T. Nakajima, Y. Honda, O. Kitao, H. Nakai, T. Vreven, K. Throssell, J. A. Montgomery, Jr., J. E. Peralta, F. Ogliaro, M. J. Bearpark, J. J. Heyd, E. N. Brothers, K. N. Kudin, V. N. Staroverov, T. A. Keith, R. Kobayashi, J. Normand, K. Raghavachari, A. P. Rendell, J. C. Burant, S. S. Iyengar, J. Tomasi, M. Cossi, J. M. Millam, M. Klene, C. Adamo, R. Cammi, J. W. Ochterski, R. L. Martin, K. Morokuma, O. Farkas, J. B. Foresman, and D. J. Fox, Gaussian, Inc., Wallingford CT, 2016.
- [24] M. Head-Gordon, J.A. People, M.J. Frisch, Chem. Phys. Lett. 153 (6) (1988) 503–506, https://doi.org/10.1016/0009-2614(88)85250-3.
- [25] A.D. Becke, Density-function thermochemistry. III. The role of exact exchange, J. Chem. Phys. 98(7) (1993) 5648-5652. DOI: 10.1063/1.464913.
- [26] R. Peverati, D.G. Truhlar, Improving the accuracy of hybrid meta-GGA density functionals by range separation, J. Phys. Chem. Lett. 2 (2011) 2810–2817, https://doi.org/10.1021/jz201170d.
- [27] G.E. Scuseria, C.L. Janssen, H.F. Schaefer III, An efficient reformulation of the closed-shell coupled cluster single and double excitation (CCSD) equations, J. Chem. Phys. 89 (12) (1988) 7382–7387, https://doi.org/10.1063/1.455269.
- [28] R.A. Kendall, T.H. Dunning Jr, R.J. Harrison, Electron affinities of the first-row atoms revisited. Systematic basis sets and wave functions, J. Chem. Phys. 96(9) (1992) 6796-6806. DOI: 10.1063/1.462569.
- [29] T.H. Dunning Jr, Gaussian basis sets for use in correlated molecular calculations. I. The atoms boron through neon and hydrogen, J. Chem. Phys. 90(2) (1989) 1007-1023. DOI: 10.1063/1.456153.
- [30] F. Weigend, F. Furche, R. Ahlrichs, Gaussian basis sets of quadruple zeta valence quality for atoms H-Kr, J. Chem. Phys. 119 (24) (2003) 12753–12762, https://doi. org/10.1063/1.1627293.
- [31] W. Li, L. Evangelisti, Q. Gou, W. Caminati, R. Meyer, The barrier to proton transfer in the dimer of formic acid: a pure rotational study, Angew. Chem., Int. Ed. Engl. 58 (2019) 859–865, https://doi.org/10.1002/anie.201812754.
- [32] Zbigniew Kisiel, "PROSPE database: Programs for ROtational SPEctroscopy,". http://info.ifpan.edu.pl/~kisiel/prospe.htm.
- [33] H. Hartwig, H. Dreizler, The Microwave Spectrum of trans-2,3-Dimethyloxirane in Torsional Excited States, Z. Naturforsch. A. 51a(8) (1996) 923-932. DOI: 10.1515/ zna-1996-0807.
- [34] S. G. Kukolich, Measurements of Ammonia Hyperfine Structure with a Two-Cavity Maser, Phys. Rev. 156, (1967) 83-92, https://doi.org/10.1103/PhysRev.156.83.